ISSN (Online) 2456-1290

International Journal of Engineering Research in Mechanical and Civil Engineering (IJERMCE)
Vol 3, Issue 3, March 2018

Role of Vane Angle and its Shape on Jet Mixing of a Subsonic Coaxial Jet

[1] Aishwarya Singh Rathore, [2] Neeraj Sharma, [3] Namita Mahindru, [4] G.Mahendra Perumal, [5] Vinayak Malhotra
[1][2][3][4] [5] Department of Aerospace Engineering, SRM Institute of Science and Technology, Kattankulathur, Tamil Nadu-603203, INDIA

***Abstract* - Noise emission control from the jet engine is one of the biggest emerging concerns for the aviation industry as well as for the defense organization. Every year, the aviation industry is facing the 1-billion-dollar loss because of the tremendous emission of noise from the aircraft engines. In future, for certification process of an aircraft, noise emission level will be set as one of the norms in the inspection. Taking into consideration this global concern, in the present investigation, a computational study was carried out to reduce the jet noise for subsonic aircraft by achieving the enhanced jet mixing rate. Computational analysis was done to study the effect of vane orientation angle and its shape on a coaxial jet. The vanes were positioned in the annular passage of the coaxial jet in the coaxial duct. The analysis was done to study the effect of vane orientation angle (0°, 10° and 30°) and vane shapes namely rectangle and a rectangle with positive fillet on a jet mixing of a subsonic coaxial jet using ANSYS16. For computational analysis, the inlet boundary condition was given as 92.1m/s along with the free slip wall condition. Results indicate that the jet mixing rate was enhanced for the vane with the positive filleted rectangular cross-section of vane angle 30°.**

***Index Terms*: Coaxial Duct, Jet Mixing, Positive Filleted Rectangular Cross Section, Vane Angle.**

I. INTRODUCTION

A flow jet refers to the fluid low coming out from an opening at high velocity. The flow jets are broadly encountered in nature and cover wide range of applications including aircraft gas turbine engines, liquid and solid rocket motors, boundary layer separation control over a wing, film cooling on turbine blades, etc. In free jet mode as the fluid moves downstream, it interacts with the surrounding fluid and its momentum drops. Consequently, the efflux of jet rifts into two distinct regions viz., a region near the centreline where fluid interacts less with the surrounding medium and maintains nearly its initial speed some distance downstream termed as the potential core or the core. The length of core region in flow jets under varying conditions is a prominent factor. Next is region outside the core where fluid comprehensively interacts with the surrounding fluid. This region is known as the entrainment region and it is identified by drastic change in flow characteristics. Co-axial jet refers to the two-different density of jets coming out from two different parallel passages sharing the same axis. One jet, being the primary flow, and the other jet, being the secondary flow. In single jets, only primary core region exists and so one shear layer formation is observed. Whereas in coaxial jets, both primary and secondary core regions can be easily distinguished and so two shear layers exist. Compared to the single free jet, the co-axial non-swirl or swirl jet, shows higher spread rate, and so more jet noise reduction is detected. Co-axial jets develop more rapidly than single jets, as potential core length is found to decrease more, indicating small axial length and more enhanced mixing rate. The co-axial jet flow is broadly classified into three zones, and the same regions can be extended for co-axial swirl jets. Fig. 1 shows the three zones of co-axial flow. The three zones are:

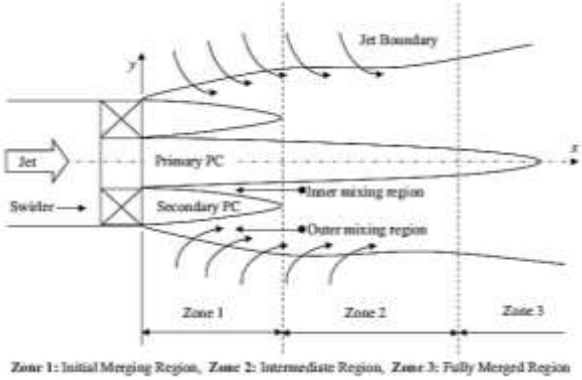

Fig.1. The three zones of co-axial flow

1) Potential Core Region: In this region, primary and secondary potential cores both exist. Potential flow characteristics are being exhibited by the flow. Inner and outer shear layers can be easily distinguished in this region.
2) Intermediate or Transition Region: Both primary and secondary potential core regions now merge together in this region. Turbulent mixing takes up intermittent character by counter rotating stream wise vortices. Turbulent mixing enhances in this region.

3) Self-Similar Region: If in this region upper half is observed, same flow properties values are obtained as for the

lower half. It just acts a mirror image. It is also known as fully merged flow region.

Following to the classical work of Broadbent [1] on shielding of engines from the ground by means of the aircraft wing and tail plane, Appreciable experimental, numerical, and analytical had been carried out to understand the heterogenous fluid flow phenomenon. Ahmed and Sharma [2], did experimental investigation of turbulent mixing of two co-axial jets with low annular to core area ratio in a non-separating confinement was being done. Mixing of jets with low area ratio was considered. Effect of velocity ratio of the two streams was studied by changing the velocity ratio from 0.3 to 10. Rate of mixing gets enhanced when the outer stream has higher velocity was declared in this paper. Joslin et. al., [3], focused both on flow control as well as noise control. Liners were incorporated inside the combustion chamber to reduce power plant noise, and structural modifications of wing were done to reduce structural noise emission. Georgiades and Debonis [4] through systematic simulations used RANS to produce small scale turbulence in wall boundary layer and LES for large scale jet mixing. RANS was declared more accurate than LES methods. NevinCelik and HaydarEren [5], investigated heat transfer characteristics of co-axial impinging jets along with the velocity field. They found that, for cooling a broad expanse of surface, co-axial jets of high d/D are preferable, and for localized cooling, the single jet (d/D=0) would perform the best. Vlasenko et. al., [6], presented a computational viewpoint on the problems of design and numerical simulation for the ducts of modern aircraft turbofan engines. The work highlighted the contribution of noise in overall noise emission from aircraft due to potential core and transition region. Xia, et. al., [7], explored efforts of using large-eddy simulation (LES) type methods to study complex and realistic geometry single stream and co-flow duct jets and acoustics. The pylon was observed to have a global effect on the circumferentially averaged flow, causing the jet mix out more quickly, have thicker shear layer near duct exit, and faster decay of peak velocity. Filippone [8], studied aircraft noise prediction by carrying out simulation. The point of view taken in this context was that of comprehensive models that couple the various aircraft systems with the acoustic sources, the propagation and the flight trajectories. Zhao and Li., [9] utilized Tunable acoustic dampers as a passive control means to stabilize combustion/engine systems by optimizing the damping effect of the dampers in response to changes in operating conditions.

Balakrishnan and Srinivasan [10], accounted enhancement in turbulent mixing for co-axial flow as one of the most significant technique in reducing noise emission. Experimental studies were carried out to reduce the jet noise using co-axial swirlers in the form of curved vanes fixed in an annular passage. Swirls produced proved to eliminate transonic tones and weak swirl proved to be more efficient for noise reduction at subsonic conditions. From the above literature, it was observed that, not much work was done on noise emission control using co-axial duct incorporated swirlers to produce swirl flow. The present work is motivated by the need to rule out one of the biggest emerging concern of the aviation industry, i.e., noise emission control from jet engines. Coaxial duct with incorporated swirlers in the form of vanes can be used, to increase the jet spread rate, which directly reduces the potential core length and so the emitted jet noise. Since swirl promotes the generation of vortices in the flow, and so higher vortex intensities will retard the axial momentum faster, thus reducing the potential core and jet lengths. Increasing the swirl number, i.e., increasing the vane angle will convert more of the axial momentum into tangential momentum, which lowers the axial velocity further after the swirl. The specific objectives of the present work are:

a) To investigate the role of vane angle on coaxial flow jet performance.

b) To explore the role of key controlling parameters.

II. COMPUTATIONAL STUDY

A systematic computational analysis was carried out to evaluate the performance alteration owing to the subjected changes. Primarily, the cross-section of the curved vanes was used to produce the swirl flow. Present work accounts, rectangular and rectangle with positive fillet cross section vanes were tested in the co-axial exhaust duct, with vane angles as 0, 10 and 30 degrees respectively. Fig.2((a) and (b)), shows the cross section of the vane incorporated coaxial duct viz., the rectangular cross section of the vane(Fig.2(a)), and the positive filleted rectangular cross section of the vane (Fig.2(b)). The models of co-axial duct with curved vanes incorporated with rectangular and positive filleted rectangular cross section were modeled using CATIA V5 and thoroughly analyzed in ANSYS 16. Models were created in CATIA V5 and imported in ANSYS 16 workbench in CFX. Models of co-axial duct with incorporated swirlers were made using CATIA software in part design module. Selected co-axial duct with 6 vanes of rectangle with positive fillet of 0.5 mm radius cross section and rectangular cross section with vane angles 0, 10, and 30 degrees were made respectively. Fig.3 shows the schematic of coaxial duct with dimensions. For the present co-axial duct model, the swirler outer diameter (Dos) was kept as 16 mm, swirler diameter(Ds) as 14 mm, outer hub diameter (Doh) as 7 mm and internal hub diameter(Dh) as 6mm respectively. The vane width(w) was kept as 6 mm and the vane thickness (t) was kept as 1mm.

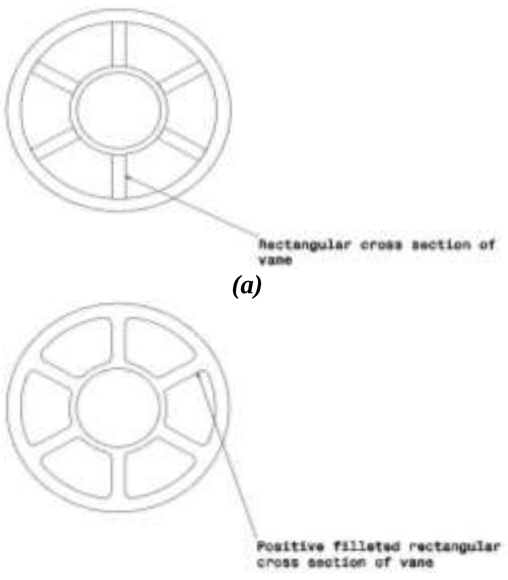

(a)

(b)

Fig.2. (a) Depiction of rectangular vane cross section and (b) positive filleted rectangular cross section of vane.

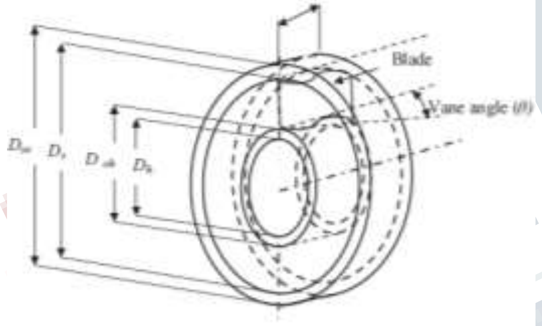

Fig.3. Dimensioning of the co-axial duct along with curved vane.

Fig.4. shows the 3D designed models of co-axial exhaust ducts with incorporated swirlers as curved vanes of rectangular and positive filleted rectangular cross section. In pre-processor, the inlet boundary condition was given as velocity as 92.113 m/s along with the 'k-Ɛ' turbulence model as. Free slip wall boundary condition was given for the duct. The fluid taken was air at 25oC. The pressure-based solver was used to solve the analysis.

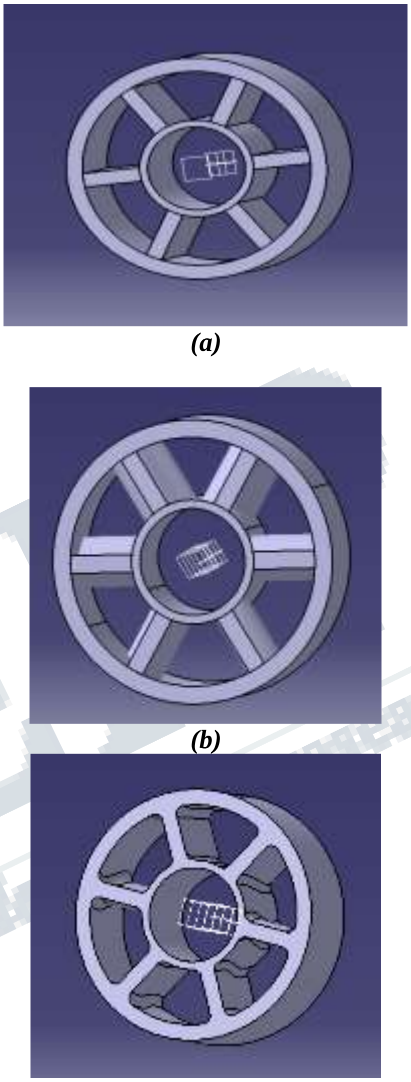

(a)

(b)

(c)

Fig.4. 3D designed models of Co-axial exhaust duct with incorporated curved vanes of rectangular and positive filleted rectangular cross section with vane angle as (a) 0° (b)10° and (c) 30°.

It is important to note that all the simuations predictions presented represent repeatability.

III. RESULTS AND DISCUSSIONS

For the co-axial duct with the fixed curved vanes with vane angle as 0°, 10° and 30°, the swirl number was calculated using the below mentioned formula:

$$S = \frac{2}{3}\left(\frac{1-(D_h/D_s)^3}{1-(D_h/D_s)^2}\right)\tan\theta$$

where, S is the swirl number produced by curved vanes of varied vane angle, Dh is the hub diameter, Ds is the swirl diameter and ɵ is the vane angle. The swirl number calculation for selected vane angles viz., 0°, 10° and 30° are shown in the Table-1. The flow regions and the jet spread were observed with contour plots of velocity for all the designed models.

VANE ANGLE	SWIRL NUMBER
0°	0
10°	0.1328
30°	0.4347

Table1: Swirl number for the respective vane angles.

Fig.5. shows the velocity contour plots obtained by computationally analyzing the co-axial exhaust duct models with incorporated curved vanes of rectangular cross section with vane angles being 0°, 10° and 30° respectively. Enhanced jet mixing was easily comparable with the contour plots obtained for all the three models. One can note from Fig.5. (c) (viz., 30°) rectangular cross section vane model, that the potential core region length was greatly reduced as compared to all the other 2 models, which directly relates to enhanced jet mixing.

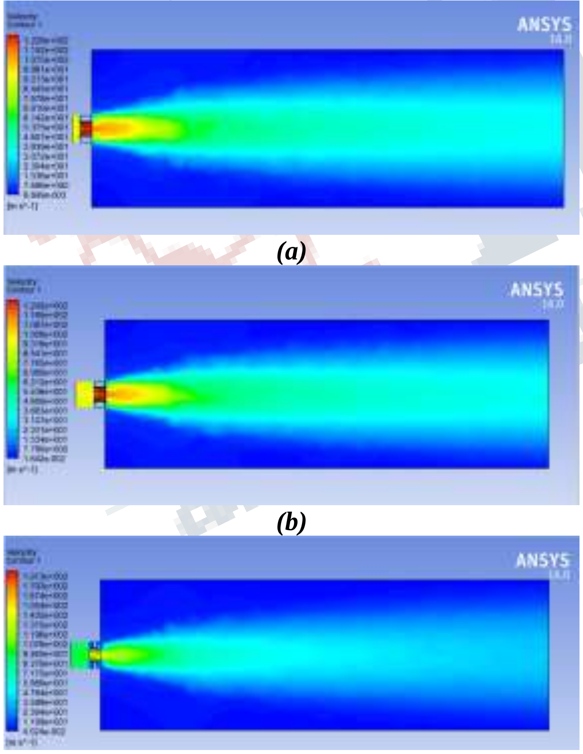

(a)

(b)

(c)

Fig.5. Velocity contour plots for computationally analyzed co-axial exhaust duct models with curved vanes of rectangular cross section with vane angles as (a) 0°, (b) 10° and (c) 30°.

The reason for above mentioned changes may be attributed to the fact that increase in the swirl number, results in enhanced axial momentum conversion into tangential momentum thus lowering the axial velocity after the swirl. The potential core length depends on the free stream velocity, and the increase in swirl was noted post the jet decay length. The above-mentioned effect occurs because of the flow expansion (radial pressure gradients) set in by the swirl, that causes enhanced flow expansion than at the low and without swirl. Swirl promotes the generation of tangential momentum along-with axial momentum. Both these momentum result in formation of shear layers and transition to vortices generation. Further, the vortex intensities are more significant compared to non-swirling case which retards the axial momentum quickly by faster diffusion and thus lowers potential core and jet lengths. The axial momentum loss gets converted to the turbulent kinetic energy, owing to steep velocity gradients, eventually resulting more mixing and reduction in noise levels.

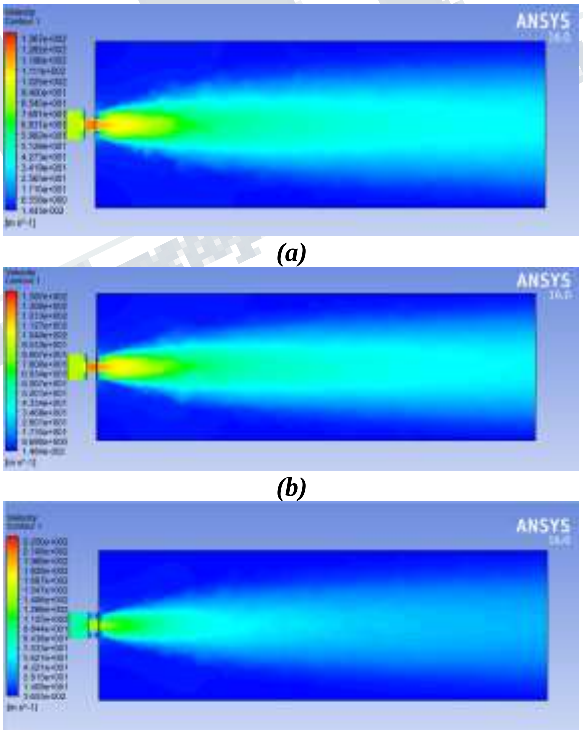

(a)

(b)

(c)

Fig.6. Velocity contour plots for computationally analyzed co-axial exhaust duct models with curved vanes of positive filleted rectangular cross section with vane angles as (a) 0°, (b) 10° and (c) 30°.

Fig.6. shows the respective velocity contour plots obtained by analyzing the co-axial exhaust duct models with incorporated curved vanes of positive filleted rectangular

cross section with vane angles. Looking at the contours, one can note that the enhanced jet mixing is easily comparable for all the three models and with the models of rectangular cross section. Comparing positive filleted rectangular cross section model with the rectangular cross section model, enhanced jet mixing was observed for the case of positive filleted rectangular cross section than for the rectangular cross section model (please see Fig. 6(c)) showing additional reduced potential core region length as compared to the other two angle models. The fillets are minute vortex generators, that cause the incoming and exiting flow (the flow before and after swirler) to be turbulent, thereby increasing the turbulent intensities and significantly reducing axial momentum resulting in lower potential core lengths, even in the absence of swirl flow. The effect of swirl is to increase the vortex intensity by a cross coupling of impinging vortices.

The impinging vortices refer to the interaction of the large scale-jet (axial) and swirl motion along with the small-scale fillet vortices. These interactions can trigger generation of vortex of greater intensities and which can lead to greater momentum diffusion. Therefore, more reduced potential core length region is achieved for the co-axial model with positive filleted rectangular cross section vane particularly for 30° vane angle, than the co-axial duct model with rectangular cross section vane.

It is important to note that for methodical calculations here, ‘Z/De’ is the ratio of velocity taken vertically starting from centre line at fixed intervals in lateral direction and the velocity at exit of the duct. ‘Z’ is the axial length along the jet center line in meters. ‘X’ is the lateral length from the jet center in meters. ‘De’ is the exit diameter taken as 14 mm. ‘X/De’ is the ratio of axial center-line velocity at fixed intervals and duct exit velocity. Fig.7. shows the comparison of the jet half width variations of co-axial jet with swirler of vane angle as 0 degree. One can note that the jet half width for rectangular cross section vane is slightly higher for some regions than the positive filleted rectangular cross section of the vane.

Careful observation of the data reveals that at 0.35De, the velocity for rectangular cross section is more than that for positive filleted rectangular cross section by 60%. As the graph progresses, at 1.05De, 1.91De, 4.9De and 10De, the two curves are noted to merge showing same velocity. At intermediate locations, velocity for rectangle amounts 11% greater than positive fillet rectangle velocity.

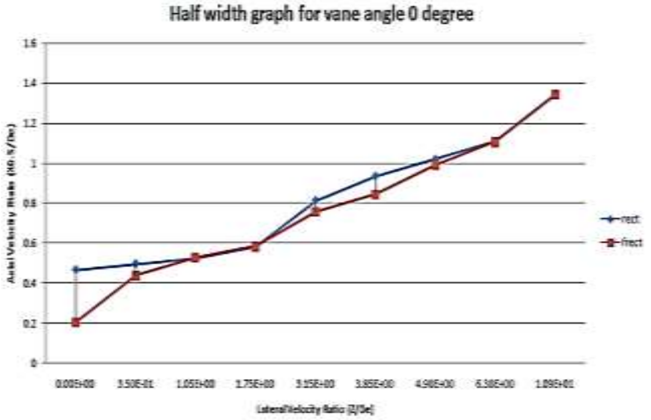

Fig.7. Half width graph for co-axial duct with swirler vane angle as 0 degree.

Next, we look at the effect of varying vane angle. Fig.8. shows the comparison of the jet half width variations of co-axial jet with swirler of vane angle as 10 degrees. The jet half width was noted to be slightly higher for filleted rectangular cross section for most of the regions than for the rectangular cross section vane. At 0.35De location, the velocity for rectangle was found to be more than that for positive filleted rectangle by 60%. At 1.03De, 1.91De, 3.15De and 3.85De the two curves merge showing same velocity is achieved for both the cross sections at those locations. At location 10De, the velocity for positive fillet rectangle was found to be more by 7% than for rectangle velocity. It is interesting to note that, for certain regions, velocity for positive fillet rectangle surpasses by more than 11% for the rectangle velocity whereas, certain configuration shows the rectangle velocity more by 7% than the positive fillet rectangle velocity. than the rectangle cross section, and thus dropping the jet noise emitted.

The study was further extended to the comparison of the jet half width variations of co-axial jet with swirler of vane angle at 30 degrees (Fig.9).

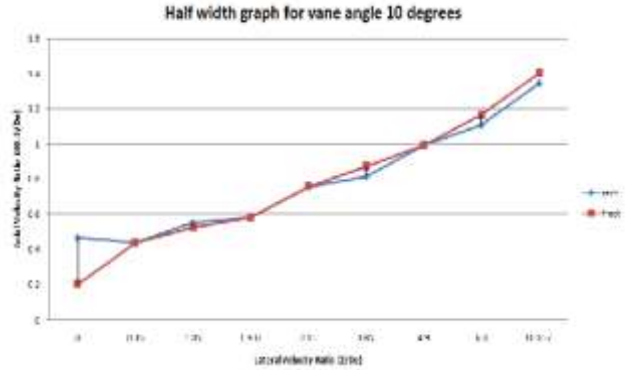

Fig.8. Half width graph for co-axial duct with swirler vane angle as 10 degrees.

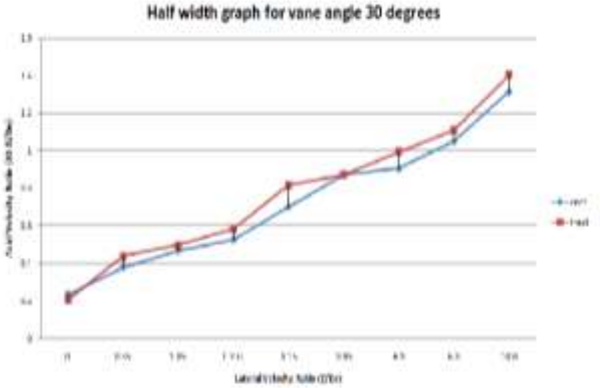

Fig.9. Half width graph for co-axial duct with swirler vane angle as 30 degrees.

Looking at the plot one can note that, the jet half width is much higher for positive filleted rectangular cross section vane than for the rectangular cross section vane. At 0.35De, the velocity for rectangle was found to be more than that for positive filleted rectangle by 13% however, the two curves merges at 3.85De, showing same velocity achieved. At 3.15De, the velocity for positive fillet rectangle was more than that for rectangle velocity by 19% and similar trend was observed at 10De, with 7% rise. Other positions report, the velocity for positive fillet rectangle to be more than the rectangle velocity by 10%. The reasons for above mentioned changes may be attributed to the dominant coupled effect of vane angle and positive fillet rectangular cross section owing to strong velocity-vorticity interactions in the shear layer than the singular vane angle effect for rectangular cross section vane. This signifies enhanced reduction in the potential core region length in positive fillet rectangle cross section.

IV. CONCLUSION

Systematic computational study was carried out for 3D co-axial exhaust duct to understand the effect of vane angle variation and fillets on jet noise. Selected cases of the co-axial exhaust duct models with swirlers as curved vanes of rectangular and positive filleted rectangular cross section with vane angles as 0°, 10° and 30° respectively were tested. Based on the investigations, it can be concluded that positive fillet rectangular cross section coupled with appropriate vane angle results in better reduction in potential core length. Larger vane angle (here 30 Degrees) results in significant growth than that for the rectangular cross sectioned vane by 20%, hence directly reducing jet noise emitted. Certain locations result in the similar velocity profile for both the cross sections and of rectangle dominating than the positive fillet rectangle. Presence of fillets prove an efficient factor in promoting better mixing. Varying vane results in providing improved velocity-vorticity induced mixing strength. However, the better enhanced mixing and so reduced jet noise emission, can be achieved for the co-axial exhaust duct model with coupled effect of curved vane and positive filleted rectangular cross section as compared to all the other models.

Applications of Present work: Coaxial duct with incorporated swirlers can be fixed at exit of the mixed turbofan engine that will enhance the mixing of jet and so reduce the jet noise emitted; burner arrangement including coaxial swirler which makes it impossible for undesired instances of ignition of the fuel-air mixture to occur outside the combustion chamber.

REFERENCES

[1] E. G. Broadbent, “Noise shielding for aircraft”, Royal Aircraft Establishment, Farnborough, Prog. Aerospace Sci, Vol. 17, pp, 231-268. Pergamon Press. Printed in Great Britain, 1977.

[2] M.R. Ahmed and S.D. Sharma, “Effect of velocity ratio on the turbulent mixing of confined, co-axial jets”, Experimental Thermal and Fluid Science, 22, 19-33, 2000.

[3] Ronald D. Joslin, Russell H. Thomas and Meelan M. Choudhari, “Synergism of flow and noise control technologies”, Progress in Aerospace Sciences, 41,363–417, 2005.

[4] Nicholas J. Georgiadis and James R. DeBonis, “Navier-stokes analysis methods for turbulent jet flows with application to aircraft exhaust ducts”, Progress in Aerospace Sciences, 42 377–418, 2006.

[5] NevinCelik and HaydarEren, “Heat transfer due to impinging co-axial jets and the jets’ fluid flow characteristics”, Experimental Thermal and Fluid Science, 33, 715–727, 2009.

[6] V. Vlasenko, S. Bosniakov, S. Mikhailov, A. Morozov and A. Troshin, “Computational approach for investigation of thrust and acoustic performances of present-day ducts”, Progress in Aerospace Sciences, 46,141–197, 2010.

[7] H. Xia, P. G. Tucker, S. Eastwood and M. Mahak, “The influence of geometry on jet plume development”, Progress in Aerospace Sciences, 52, 56–66, 2012.

[8] Antonio Filippone, “Aircraft noise prediction”, Progress in Aerospace Sciences, 68, 27-63, 2014.

[9] Dan Zhao and X. Y. Li, “A review of acoustic dampers applied to combustion chambers in aerospace industry”, Progress in Aerospace Sciences, 74, 114–130, 2015.

[10] P. Balakrishnan and K. Srinivasan, “Jet noise reduction using co-axial swirl flow with curved vanes”, Applied Acoustics, 126, 149–161, 2017